Original Article

Correlation of *In Vivo* and *In Vitro* Methods in Measuring Choroidal Vascularization Volumes Using a Subretinal Injection Induced Choroidal Neovascularization Model

Chuang Nie[1], Mao-Nian Zhang[1], Hong-Wei Zhao[2], Thomas D Olsen[3], Kyle Jackman[3], Lian-Na Hu[2], Wen-Ping Ma[4], Xiao-Fei Chen[1], Juan Wang[4], Ying Zhang[1], Tie-Shan Gao[2], Hiro Uehara[3], Balamurali K Ambati[3], Ling Luo[2]

[1]Department of Ophthalmology, Chinese PLA General Hospital, Beijing 100853, China
[2]Department of Ophthalmology, The 306th Hospital of PLA, Beijing 100101, China
[3]Moran Eye Center, University of Utah, Salt Lake City, Utah 84132, USA
[4]Department of Ophthalmology, The 261th Hospital of PLA, Beijing 100094, China

Abstract

Background: *In vivo* quantification of choroidal neovascularization (CNV) based on noninvasive optical coherence tomography (OCT) examination and *in vitro* choroidal flatmount immunohistochemistry stained of CNV currently were used to evaluate the process and severity of age-related macular degeneration (AMD) both in human and animal studies. This study aimed to investigate the correlation between these two methods in murine CNV models induced by subretinal injection.

Methods: CNV was developed in 20 *C57BL6/j* mice by subretinal injection of adeno-associated viral delivery of a short hairpin RNA targeting sFLT-1 (AAV.shRNA.sFLT-1), as reported previously. After 4 weeks, CNV was imaged by OCT and fluorescence angiography. The scaling factors for each dimension, x, y, and z (μm/pixel) were recorded, and the corneal curvature standard was adjusted from human (7.7) to mice (1.4). The volume of each OCT image stack was calculated and then normalized by multiplying the number of voxels by the scaling factors for each dimension in Seg3D software (University of Utah Scientific Computing and Imaging Institute, available at *http://www.sci.utah.edu/cibc-software/seg3d.html*). Eighteen mice were prepared for choroidal flatmounts and stained by CD31. The CNV volumes were calculated using scanning laser confocal microscopy after immunohistochemistry staining. Two mice were stained by Hematoxylin and Eosin for observing the CNV morphology.

Results: The CNV volume calculated using OCT was, on average, 2.6 times larger than the volume calculated using the laser confocal microscopy. The correlation statistical analysis showed OCT measuring of CNV correlated significantly with the *in vitro* method ($R^2 = 0.448$, $P = 0.001$, $n = 18$). The correlation coefficient for CNV quantification using OCT and confocal microscopy was 0.693 ($n = 18$, $P = 0.001$).

Conclusions: There is a fair linear correlation on CNV volumes between *in vivo* and *in vitro* methods in CNV models induced by subretinal injection. The result might provide a useful evaluation of CNV both for the studies using CNV models induced by subretinal injection and human AMD studies.

Key words: Choroidal Flatmount; Choroidal Neovascularization; Correlation; Spectral-domain Optical Coherence Tomography

Introduction

Exudative age-related macular degeneration (AMD) is a primary cause of blindness in industrialized countries.[1] It is characterized by choroidal neovascularization (CNV) and is associated with the growth of fibrovascular tissue from the choriocapillaris through defects in Bruch's membrane into the subretinal space.[2-4] Clinicians evaluate and follow up CNV after treatment primarily by optical coherence tomography (OCT), which demonstrates retinal morphology such as thickness and structure. Therefore, *in vivo* volumetric analysis of CNV based on OCT examination is indispensable to evaluate CNV lesion changes accurately in experimental studies.

Over the past 20 years, OCT produces cross-sectional images of tissue structures noninvasively based on its optical reflectivity.[5] OCT imaging has had a dramatic impact on the diagnosis and management of AMD and the other vitreoretinal disease.[5-11] The software of OCT which can measure the retinal thicknesses for a human is reported

Access this article online

Quick Response Code:

Website: www.cmj.org

DOI: 10.4103/0366-6999.157681

Address for correspondence: Dr. Ling Luo, Department of Ophthalmology, The 306th Hospital of PLA, Beijing 100101, China
E-Mail: Ling.luoling1208@gmail.com
Dr. Balamurali K Ambati, Moran Eye Center, University of Utah, Salt Lake City, Utah 84132, USA
E-Mail: bambati@gmail.com

previously,[12] and subsequently is widely used to measure neovascular AMD, retinal and choroidal neovascular diseases in animal studies.[13-17]

Laser-induced rupture of Bruch's membrane in mice is widely used in CNV animal studies, which is in good agreement with a histological section in animal studies.[16,18] However, it has many differences from human exudative AMD.[19] Laser-induced CNV has short duration, less retinal edema, and spontaneous retinal pigment epithelium (RPE) recovery and CNV regression rapidly that all contrast to human AMD-related CNV and set the limitations of this model for interventional studies.[16]

Choroidal neovascularization volumes calculated by laser confocal microscopy combined with immunostaining *in vitro* using ImageJ software (developed by Wayne Rasband, National Institutes of Health, Bethesda, MD, USA; available at *http://rsb.info.nih.gov/ij/index.html*) currently is also widely used in animal CNV studies.[20,21] However, this method only can be used after the animal euthanized, and the CNV baseline cannot be evaluated, and the CNV volumes only were calculated from CNV due to lose partial retinal CNV tissues.[22] Recently, some researchers also used OCT combined with ImageJ software to calculate the CNV volumes *in vivo*.[23,24] Giani *et al*.[23] got a fair correlation between CNV volume obtained with choroidal flatmounts and OCT in laser-induced CNV model.

Many researchers also have developed CNV animal models induced by subretinal injection that document an increase in CNV size for a long time and mimic human AMD.[25-27] Luo *et al*.[28,29] evaluated the CNV volumes by using OCT in subretinal injection-induced CNV model. However, to our knowledge, the correlation of CNV between *in vivo* and *in vitro* methods in subretinal injection animal studies has not been reported. In this study, we investigated the comparability and correlation of OCT *in vivo* and histological methods *in vitro* for quantifying subretinal injection-induced CNV volumes.

Methods

Mice

C57BL/6J mice were obtained from Chinese PLA General Hospital. Experimental groups were age and sex matched. A total of 20 healthy mice (age: 6–8 weeks) were used in this study. Eighteen mice were used for measuring CNV volumes, the remaining two mice were for histological analysis. All procedures conformed to the Association for Research in Vision and Ophthalmology Statement on Animal Research.

Choroidal neovascularization models induced by subretinal injection

Mice were anesthetized intraperitoneally using 10% chloral hydrate (0.3 ml/100 g, The 306th Hospital of PLA), and pupils were dilated with topical tropicamide ophthalmic solution (SANTEN OY Incorporated, Japan). Under the stereomicroscope (Zeiss, Germany), a small incision was made at the pars plana of right eye, the 33 gauge syringe (Hamilton, USA) loaded with AAV.shRNA.sFLT-1 (1 μl, 1.4×10^{11} genomic copies/ml, developed as previously described[30]), was inserted through the incision, vitreous, into the subretinal space.[28] Visualizing a retinal bleb as retinal detachment proved successful subretinal delivery. Mice that developed intraocular hemorrhage during the procedure were excluded from this study because 100% of eyes had CNV regardless of the material injected.[26]

Choroidal neovascularization images acquired *in vivo*

Four weeks after surgery, mice (n = 20) were anesthetized, and the pupils were dilated. All *in vivo* imaging described was performed using a Spectralis Heidelberg Retina and OCT (HRA + OCT) system (Heidelberg Engineering Inc., Vista, CA, USA). Mice were intraperitoneally injected with 0.1 ml 10% sodium fluorescein (Alcon, Alcon Laboratories, Incorporated; USA) and observed using fluorescence angiography (FA) and OCT mode. CNV was evaluated by a combination of images obtained by FA and cross-sectional OCT.

In vivo quantification of choroidal neovascularization volume

Choroidal neovascularization volumes were measured as described previously in a blind manner, and each method was completed by one person.[28] Briefly, the corneal curvature standard, which is designed for the human eye (7.7), was adjusted to the parameters for a murine eye (1.4). OCT image stacks (3.87 μm slices) were exported from the Spectralis database and uploaded to Seg3D software (University of Utah Scientific Computing and Imaging Institute, available at *http://www.sci.utah.edu/cibc-software/seg3d.html*). For each OCT image within each stack, the CNV area on each two-dimensional image was outlined sequentially, and the software generated a figure indicating the number of voxels covered by the region of interest. The CNV volume was calculated by adding voxel values for all the images within each stack and standardizing that voxel volume value by multiplying it by the scaling factor for each dimension.

Measuring the volumes of choroidal neovascularization in flatmount

After imaging by OCT, eyes of eighteen mice were enucleated immediately and fixed with 4% paraformaldehyde (PFA) for 60 min at 4°C. Under a dissecting microscope, we removed anterior segments and then washed eye cup three times in phosphate-buffered saline (PBS). And the neurosensory retinas were gently detached and separated from the optic nerve. Four relaxing radial incisions were made, the remaining RPE-choroid-sclera complex was blocking with buffer (containing 1% bovine serum albumin; Sigma, USA) and 0.5% Triton X-100 (Sigma-Aldrich) for 60 min at room temperature, then were incubated overnight with anti-mouse CD31 antibody (an endothelial marker of new blood vessels) (1:200, Abcam, USA) at 4°C. After washing three times with PBS, and then secondary antibodies, which were conjugated to Cy3-Labeled Goat anti-rabbit

IgG (1:1000, Immunol Fluorence Staining Kit, Beyotime, Shanghai, China), were added to visualize for 60 min. The slides were then washed three times with PBS and coverslipped. Flatmounts were examined and photographed using an Axiovert 200 microscope (Zeiss, Germany) equipped with confocal epifluorescence illumination. The area of CNV-related fluorescence was measured. Horizontal optical sections (3.87 μm) were obtained from the surface of the RPE-choroid-sclera complex. CNV was identified by setting a threshold level of fluorescence above which only vessels were captured. The cross-sectional area of the CNV images was digitally stored. The summation of the whole fluorescent area in each horizontal section was used as an index for the volume of CNV, as described previously.[20,21] The area of CNV-related fluorescence was measured by ImageJ software.

Histological analysis

Afterward, two retinal injection-bearing mice eyes (the left eye as control group) were enucleated and subsequently fixed in 4% PFA for 2 h at 4°C, dehydrated in 30% sucrose overnight and frozen in OCT medium. Seven micrometer-thick cryosections were mounted on slides and stained with Hematoxylin and Eosin.

Statistical analysis

SPSS 13.0 (SPSS, Inc., Chicago, IL, USA) was used for statistical analysis. Paired sample *t*-test was used to analyze significant differences in CNV volumes from each method. Linear regression was used to test the statistic correlation and the average difference between the two methods. The data of CNV volumes were presented as mean ± standard deviation (SD), and $P < 0.05$ was considered to be statistically significant.

Results

Imaging of subretinal injection induce-choroidal neovascularization

Fluorescence angiography

At 4 weeks after injection, the fluorescein leakage was initially invisible during the early stage of arterial phase but increased steadily thereafter. The boundary became blurred because of dye leakage in the late phase [Figure 1a]. Same CNV lesion at flatmounts was immunostained and continuously imaged using laser confocal microscopy [Figure 1b and 1c].

Optical coherence tomography

Distinct longitudinal retinal morphologic changes were evaluated by OCT after retinal injection-induced CNV. The lesion was easily distinguished from the surrounding retina on OCT. A subretinal spindle-shaped hyper-reflective lesion represented the development of neovascularization [Figure 1d and 1e], yellow area was lined as CNV lesion using polyline tool [Figure 1f and 1g]. And the three-dimensional image showed z, y, and x axis, respectively [Figure 1h]. Sometimes, subretinal exudations appeared far from injection areas [Figure 2a]. And signs of subretinal fluid accumulation appeared in most lesion areas on OCT. Subretinal fluid was located either beneath the photoreceptor's outer or inner segment (photoreceptor layer) [Figure 2b], or very rarely inside of the outer nuclear layer, or at both sites was detected by OCT. As reported previously,[29] this model of CNV progression mimicked the pathological process of human CNV.

Hematoxylin and Eosin staining

Histological evaluation showed CNV lesion–a prominent subretinal fibrovascular complex, surrounded by proliferating RPE cells that corresponded to the hyper-reflective layers at the CNV in OCT images. The pathology change of the histological sections showed a spindle-shaped lesion [Figure 3a, yellow arrow], which exhibited a hyper-reflective outline in OCT [Figure 3b-3d, yellow arrow].

Volumes of choroidal neovascularization quantified by two methods

Choroidal neovascularization boundary was identified by OCT. The CNV volumes calculated by Seg3D software based on the OCT image stacks were $3.23 \times 106 \pm 1.85$ μm^3 [Table 1, Figure 4].

Confocal and fluorescence microscopy of choroidal flatmounts staining with CD31-stainable endothelial structures showed a clear irregular delineation of CNV lesions. The volume calculated by the ImageJ software was $1.22 \times 106 \pm 0.855$ μm^3 [Table 1, Figure 4] in choroidal flatmounts.

For the same CNV lesion, CNV volume calculated using OCT based on Spectralis microscope images was, on average, 2.6 times larger than the volume calculated using the ImageJ software in the laser confocal microscopy [Figure 4].

Table 1: Choroidal neovascularization volumes from the two methods (mean ± SD, μm^3, $n = 18$)

Mice No.	OCT	Flatmount
1	3588081.82	952606.56
2	4655949.90	1817910.71
3	3799683.41	2004576.70
4	4493993.81	1667093.99
5	1662414.86	1045501.41
6	3672122.11	1526684.94
7	4525756.49	310395.73
8	925839.70	435395.75
9	1408541.86	319654.77
10	1588864.12	231523.75
11	2503012.10	662006.43
12	3200276.33	1833295.87
13	8696038.86	2405314.69
14	3013383.87	1429097.88
15	1499834.35	482819.23
16	1707033.73	398180.50
17	2437213.70	1176554.73
18	4763803.52	3337654.04
Mean	3230102.48	1224237.10
SD	1854780.90	855455.62

SD: Standard deviation; OCT: Optical coherence tomography.

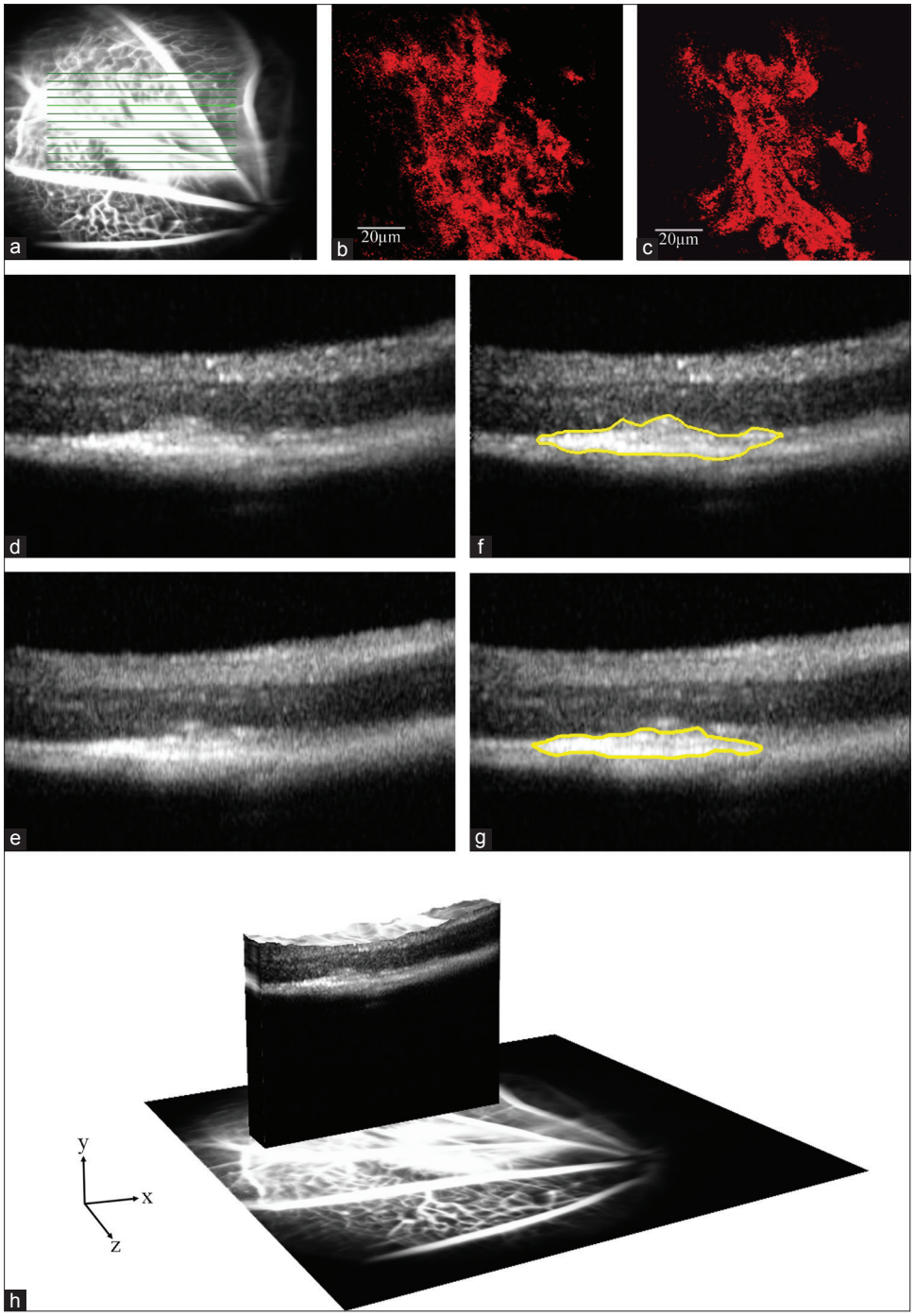

Figure 1: Choroidal neovascularization (CNV) lesion images were taken and marked for volumes calculation using optical coherence tomography (OCT) combined with Seg3D software. Fluorescence angiography (a) and OCT (d and e) images of the CNV lesion area were continuously taken by OCT; Same CNV lesion at choroidal flatmount was immunostained and continuously imaged using laser confocal microscopy (b and c). Yellow line was lined as CNV lesion using polyline tool (f and g); The three-dimensional image showed z, y, and x axis, respectively (h).

In vivo calculations of choroidal neovascularization volume using optical coherence tomography correlated with *in vitro* calculations using confocal microscopy

We compared CNV volumes obtained from *in vivo* with corresponding volumes from *in vitro* at 4 weeks after the injection. There existed a correlation between CNV volumes measured by OCT and flatmounts (R^2 = 0.448, P = 0.001, n = 18). The correlation coefficient for CNV quantification using OCT and confocal microscopy was 0.693 (n = 18, P = 0.001) [Figure 5].

Discussion

Our study indicated that a linear correlation between *in vivo* and *in vitro* methods and the correlation coefficient was 0.693. It meant that the CNV volumes calculated by OCT *in vivo*

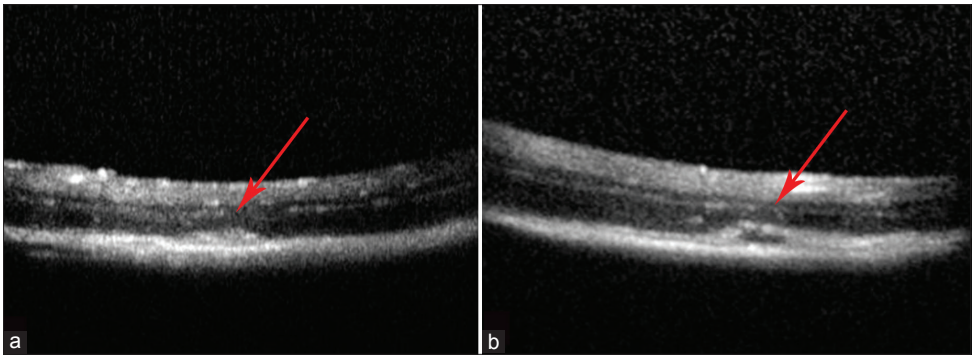

Figure 2: Besides classic choroidal neovascularization (CNV), exudations ([a] arrow), and subretinal fluid ([b] arrow) were found in the retina far from injection site of subretinal AAV.shRNA.sFLT-1 mice models, which were proved closely mimics human CNV in previous studies.

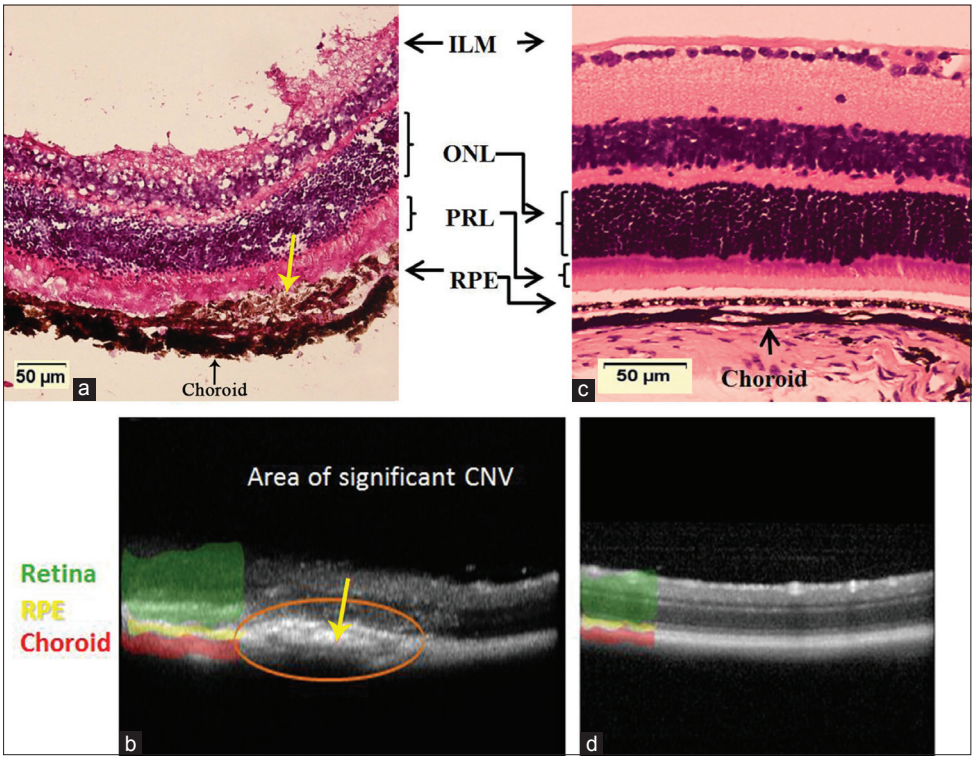

Figure 3: The subretinal injection-induced choroidal neovascularization (a and b) and normal structure (c and d) were presented by Hematoxylin and Eosin staining and optical coherence tomography. RPE: Retinal pigment epithelium; PRL: Photoreceptor's outer and inner segment; ONL: Outer nuclear layer; ILM: Internal limiting membrane.

method was fairly consistent with that by *in vitro*. Similarly, Giani *et al*.[23] investigated the correlation coefficient and their results showed 0.635 (at day 5), 0.682 (at day 7) in laser models, respectively, indicating that OCT can estimate the CNV volumes both in subreinal injection-induced CNV model and laser-induced CNV model.

In our model, the CNV volumes acquired by OCT *in vivo* were 2.6 times larger than the volumes in choroidal flatmount *in vitro*. We speculated that the difference might be the following reasons: (1) Intraretinal CNV was removed during flatmount preparation; (2) another contributing factor was that CNV calculation using the immunostaining by endothelial cell marker (CD31) reflected only the vessels in CNV complex, but without other tissues such as fibrosis. Comparably, OCT reflected not only CNV but also fibrosis tissue, edema, subretinal fluid, and all other components in CNV lesion. Hence, each of the above two methods has its own superiorities. However, quantification of CNV volumes based on OCT images still showed some advantages compared to that of CNV volumes quantified by flatmounts: (1) This *in vivo* method is noninvasive; (2) it can normalize the baseline CNV volumes by comparing pre- and post-intervention in same animal, avoiding the possible significant different baseline in different animals. Therefore, quantification of CNV volumes by OCT is suitable for the studies of comparing pre- and post-treatment, both in animal and clinic studies.

In addition, the corneal curvature standard should be adjusted according to the animal species in animal studies. However, as we know, no adjustment was made in previous studies.

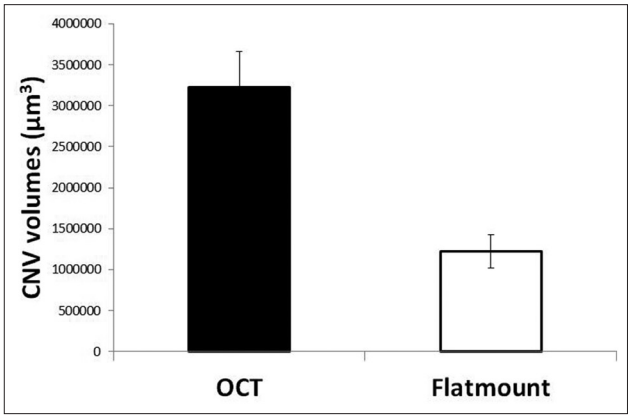

Figure 4: The choroidal neovascularization volumes were calculated by optical coherence tomography and the flatmount in the laser confocal microscopy, respectively.

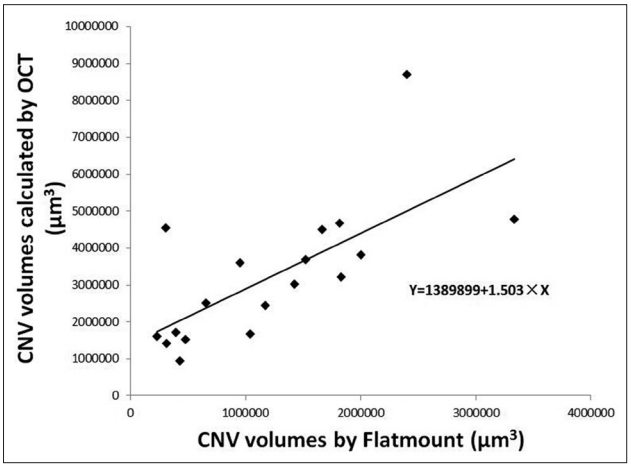

Figure 5: The correlation was analyzed between two methods for calculating the choroidal neovascularization volumes.

Some human and animal studies have demonstrated that image lateral magnification and structural measurements be affected by corneal curvature.[31-35] Therefore, we changed the corneal radius of curvature standard from 7.7 (for human) to 1.4 (for *C57BL/6J* mice)[36] in this study when processing the calculation using OCT so that the results could reach the true volumes.

Furthermore, to the best of our knowledge, our study is the first study to compare CNV volumes measured by OCT to flatmounts by CD31 staining in subretinal injection model. Unlike laser-induced CNV which could be regressed by itself quickly and hardly present retinal edema,[16] these CNV lesions showed both subretinal fluid, edema, classic CNV that resembled crucial features of neovascular AMD in humans with regard to its progression, chronicity, and morphology.[29,37] Therefore, our results might provide a useful evaluation for the studies using subretinal injection-induced CNV models. In addition, it is very crucial to identify properly the outline of CNV when using OCT following up the CNV changes. In this experiment, we excluded the hemorrhage and intraretinal or subretinal fluid, but involved fibrosis as it is hard to be distinguished completely from CNV membrane when the lesion was mixed by neurovascular and fibrosis membrane. At this point, our results might provide a useful evaluation on the size of CNV lesion for those models with similar morphological characteristics.

There are some limitations in our experiments: (1) The deeper intrachoroidal CNV could not be completely involved and imaged due to the technologic limits of Spectralis HRA + OCT imaging system; (2) since the correlation coefficient in different time point is different due to CNV lesion changed timely in laser models,[23] it is possible that correlation coefficient changed by time in subretinal injection-induced CNV models. Therefore, real-time measurement by OCT that could view the whole choroid should be further studied in the future to overcome the above limitations.

In summary, our results showed a fair linear correlation between *in vivo* and *in vitro* methods in subretinal injection-induced CNV models. These results would be helpful for CNV observation and analysis in animal studies, as well as for the operation on the patients with CNV.

References

1. Gehrs KM, Anderson DH, Johnson LV, Hageman GS. Age-related macular degeneration – emerging pathogenetic and therapeutic concepts. Ann Med 2006;38:450-71.
2. Coleman HR, Chan CC, Ferris FL 3rd, Chew EY. Age-related macular degeneration. Lancet 2008;372:1835-45.
3. Bunce C, Xing W, Wormald R. Causes of blind and partial sight certifications in England and Wales: April 2007-March 2008. Eye (Lond) 2010;24:1692-9.
4. Nagai N, Kubota S, Tsubota K, Ozawa Y. Resveratrol prevents the development of choroidal neovascularization by modulating AMP-activated protein kinase in macrophages and other cell types. J Nutr Biochem 2014;25:1218-25.
5. Huang D, Swanson EA, Lin CP, Schuman JS, Stinson WG, Chang W, *et al.* Optical coherence tomography. Science 1991;254:1178-81.
6. Puliafito CA, Hee MR, Lin CP, Reichel E, Schuman JS, Duker JS, *et al.* Imaging of macular diseases with optical coherence tomography. Ophthalmology 1995;102:217-29.
7. Rogers AH, Martidis A, Greenberg PB, Puliafito CA. Optical coherence tomography findings following photodynamic therapy of choroidal neovascularization. Am J Ophthalmol 2002;134:566-76.
8. Massin P, Duguid G, Erginay A, Haouchine B, Gaudric A. Optical coherence tomography for evaluating diabetic macular edema before and after vitrectomy. Am J Ophthalmol 2003;135:169-77.
9. Chen J, Lee L. Clinical applications and new developments of optical coherence tomography: An evidence-based review. Clin Exp Optom 2007;90:317-35.
10. Kashani AH, Keane PA, Dustin L, Walsh AC, Sadda SR. Quantitative subanalysis of cystoid spaces and outer nuclear layer using optical coherence tomography in age-related macular degeneration. Invest Ophthalmol Vis Sci 2009;50:3366-73.
11. Zheng Y, Sahni J, Campa C, Stangos AN, Raj A, Harding SP. Computerized assessment of intraretinal and subretinal fluid regions in spectral-domain optical coherence tomography images of the retina. Am J Ophthalmol 2013;155:277-86.e1.
12. Silva MF, Mateus C, Reis A, Nunes S, Fonseca P, Castelo-Branco M. Asymmetry of visual sensory mechanisms: Electrophysiological, structural, and psychophysical evidences. J Vis 2010;10:26.
13. Huber G, Beck SC, Grimm C, Sahaboglu-Tekgoz A, Paquet-Durand F, Wenzel A, *et al.* Spectral domain optical coherence tomography in mouse models of retinal degeneration. Invest Ophthalmol Vis Sci 2009;50:5888-95.
14. Gabriele ML, Ishikawa H, Schuman JS, Bilonick RA, Kim J,

Kagemann L, *et al.* Reproducibility of spectral-domain optical coherence tomography total retinal thickness measurements in mice. Invest Ophthalmol Vis Sci 2010;51:6519-23.
15. Knott EJ, Sheets KG, Zhou Y, Gordon WC, Bazan NG. Spatial correlation of mouse photoreceptor-RPE thickness between SD-OCT and histology. Exp Eye Res 2011;92:155-60.
16. Hoerster R, Muether PS, Vierkotten S, Schröder S, Kirchhof B, Fauser S. *In-vivo* and *ex-vivo* characterization of laser-induced choroidal neovascularization variability in mice. Graefes Arch Clin Exp Ophthalmol 2012;250:1579-86.
17. Groh J, Stadler D, Buttmann M, Martini R. Non-invasive assessment of retinal alterations in mouse models of infantile and juvenile neuronal ceroid lipofuscinosis by spectral domain optical coherence tomography. Acta Neuropathol Commun 2014;2:54.
18. Liu T, Hui L, Wang YS, Guo JQ, Li R, Su JB, *et al. In-vivo* investigation of laser-induced choroidal neovascularization in rat using spectral-domain optical coherence tomography (SD-OCT). Graefes Arch Clin Exp Ophthalmol 2013;251:1293-301.
19. Ryan SJ. The development of an experimental model of subretinal neovascularization in disciform macular degeneration. Trans Am Ophthalmol Soc 1979;77:707-45.
20. Ashikari M, Tokoro M, Itaya M, Nozaki M, Ogura Y. Suppression of laser-induced choroidal neovascularization by nontargeted siRNA. Invest Ophthalmol Vis Sci 2010;51:3820-4.
21. Kami J, Muranaka K, Yanagi Y, Obata R, Tamaki Y, Shibuya M. Inhibition of choroidal neovascularization by blocking vascular endothelial growth factor receptor tyrosine kinase. Jpn J Ophthalmol 2008;52:91-8.
22. Fischer MD, Huber G, Paquet-Durand F, Humphries P, Redmond TM, Grimm C, *et al. In vivo* assessment of rodent retinal structure using spectral domain optical coherence tomography. Adv Exp Med Biol 2012;723:489-94.
23. Giani A, Thanos A, Roh MI, Connolly E, Trichonas G, Kim I, *et al. In vivo* evaluation of laser-induced choroidal neovascularization using spectral-domain optical coherence tomography. Invest Ophthalmol Vis Sci 2011;52:3880-7.
24. Pennesi ME, Michaels KV, Magee SS, Maricle A, Davin SP, Garg AK, *et al.* Long-term characterization of retinal degeneration in rd1 and rd10 mice using spectral domain optical coherence tomography. Invest Ophthalmol Vis Sci 2012;53:4644-56.
25. Cao J, Zhao L, Li Y, Liu Y, Xiao W, Song Y, *et al.* A subretinal matrigel rat choroidal neovascularization (CNV) model and inhibition of CNV and associated inflammation and fibrosis by VEGF trap. Invest Ophthalmol Vis Sci 2010;51:6009-17.
26. Baba T, Bhutto IA, Merges C, Grebe R, Emmert D, McLeod DS, *et al.* A rat model for choroidal neovascularization using subretinal lipid hydroperoxide injection. Am J Pathol 2010;176:3085-97.
27. Lyzogubov VV, Tytarenko RG, Liu J, Bora NS, Bora PS. Polyethylene glycol (PEG)-induced mouse model of choroidal neovascularization. J Biol Chem 2011;286:16229-37.
28. Luo L, Uehara H, Zhang X, Das SK, Olsen T, Holt D, *et al.* Photoreceptor avascular privilege is shielded by soluble VEGF receptor-1. Elife 2013;2:e00324.
29. Luo L, Zhang X, Hirano Y, Tyagi P, Barabás P, Uehara H, *et al.* Targeted intraceptor nanoparticle therapy reduces angiogenesis and fibrosis in primate and murine macular degeneration. ACS Nano 2013;7:3264-75.
30. Ambati BK, Nozaki M, Singh N, Takeda A, Jani PD, Suthar T, *et al.* Corneal avascularity is due to soluble VEGF receptor-1. Nature 2006;443:993-7.
31. Hwang YH, Kim YY. Correlation between optic nerve head parameters and retinal nerve fibre layer thickness measured by spectral-domain optical coherence tomography in myopic eyes. Clin Experiment Ophthalmol 2012;40:713-20.
32. Patel NB, Garcia B, Harwerth RS. Influence of anterior segment power on the scan path and RNFL thickness using SD-OCT. Invest Ophthalmol Vis Sci 2012;53:5788-98.
33. Savini G, Barboni P, Parisi V, Carbonelli M. The influence of axial length on retinal nerve fibre layer thickness and optic-disc size measurements by spectral-domain OCT. Br J Ophthalmol 2012;96:57-61.
34. Lozano DC, Twa MD. Development of a rat schematic eye from *in vivo* biometry and the correction of lateral magnification in SD-OCT imaging. Invest Ophthalmol Vis Sci 2013;54:6446-55.
35. Myers CE, Klein BE, Meuer SM, Swift MK, Chandler CS, Huang Y, *et al.* Retinal thickness measured by spectral-domain optical coherence tomography in eyes without retinal abnormalities: The beaver dam eye study. Am J Ophthalmol 2015;159:445-56.e1.
36. Schmucker C, Schaeffel F. A paraxial schematic eye model for the growing C57BL/6 mouse. Vision Res 2004;44:1857-67.
37. Donoso LA, Kim D, Frost A, Callahan A, Hageman G. The role of inflammation in the pathogenesis of age-related macular degeneration. Surv Ophthalmol 2006;51:137-52.

Received: 13-02-2015 **Edited by:** Xin Chen
How to cite this article: Nie C, Zhang MN, Zhao HW, Olsen TD, Jackman K, Hu LN, Ma WP, Chen XF, Wang J, Zhang Y, Gao TS, Uehara H, Ambati BK, Luo L. Correlation of *In Vivo* and *In Vitro* Methods in Measuring Choroidal Vascularization Volumes Using a Subretinal Injection Induced Choroidal Neovascularization Model. Chin Med J 2015;128:1516-22.
Source of Support: Nil. **Conflict of Interest:** None declared.